Mira Ham,[1] Sung Sik Choe,[1] Kyung Cheul Shin,[1] Goun Choi,[1] Ji-Won Kim,[2] Jung-Ran Noh,[3] Yong-Hoon Kim,[3] Je-won Ryu,[4] Kun-Ho Yoon,[2] Chul-Ho Lee,[3] and Jae Bum Kim[1]

Glucose-6-Phosphate Dehydrogenase Deficiency Improves Insulin Resistance With Reduced Adipose Tissue Inflammation in Obesity

Diabetes 2016;65:2624–2638 | DOI: 10.2337/db16-0060

Glucose-6-phosphate dehydrogenase (G6PD), a rate-limiting enzyme of the pentose phosphate pathway, plays important roles in redox regulation and de novo lipogenesis. It was recently demonstrated that aberrant upregulation of G6PD in obese adipose tissue mediates insulin resistance as a result of imbalanced energy metabolism and oxidative stress. It remains elusive, however, whether inhibition of G6PD in vivo may relieve obesity-induced insulin resistance. In this study we showed that a hematopoietic G6PD defect alleviates insulin resistance in obesity, accompanied by reduced adipose tissue inflammation. Compared with wild-type littermates, G6PD-deficient mutant ($G6PD^{mut}$) mice were glucose tolerant upon high-fat-diet (HFD) feeding. Intriguingly, the expression of NADPH oxidase genes to produce reactive oxygen species was alleviated, whereas that of antioxidant genes was enhanced in the adipose tissue of HFD-fed $G6PD^{mut}$ mice. In diet-induced obesity (DIO), the adipose tissue of $G6PD^{mut}$ mice decreased the expression of inflammatory cytokines, accompanied by downregulated proinflammatory macrophages. Accordingly, macrophages from $G6PD^{mut}$ mice greatly suppressed lipopolysaccharide-induced proinflammatory signaling cascades, leading to enhanced insulin sensitivity in adipocytes and hepatocytes. Furthermore, adoptive transfer of $G6PD^{mut}$ bone marrow to wild-type mice attenuated adipose tissue inflammation and improved glucose tolerance in DIO. Collectively, these data suggest that inhibition of macrophage G6PD would ameliorate insulin resistance in obesity through suppression of proinflammatory responses.

In obese adipose tissue, chronic low-grade inflammation has been implicated in metabolic dysregulation and insulin resistance (1,2). Compared with lean subjects, in obese subjects adipose tissue promotes macrophage recruitment and cross-talk between adipocytes and macrophages, resulting in adipose tissue inflammation accompanied by high levels of inflammatory cytokines such as tumor necrosis factor-α (TNF-α), interleukin (IL)-1β, IL-6, and MCP-1 (1–3). Proinflammatory cytokines secreted by inflamed adipose tissue repress insulin action in metabolic organs by activating stress-induced kinases such as IκB kinase-β and Jun N-terminal kinase (JNK), which leads to systemic insulin resistance (4–6). Moreover, increased oxidative stress in obese adipose tissue contributes to adipose tissue inflammation via activation of mitogen-activated protein kinases (MAPKs) including JNK and p38 (7,8). In addition, elevated cellular levels of reactive oxygen species (ROS) further stimulate proinflammatory gene expression via the activation of nuclear factor-κB (NF-κB) pathways in obesity (7–10). It has been suggested that one of the major sources of cellular ROS in obese adipose tissue is pro-oxidative enzymes, including NADPH oxidase (9–11). Various pro-oxidative enzymes are known to be augmented in the adipose tissues of obese animals, whereas antioxidative

[1]Department of Biological Sciences, Institute of Molecular Biology and Genetics, National Creative Research Initiatives Center for Adipose Tissue Remodeling, Seoul National University, Seoul, Korea
[2]Department of Endocrinology and Metabolism, College of Medicine, The Catholic University of Korea, Seoul, Korea
[3]Laboratory Animal Resource Center, Korea Research Institute of Bioscience and Biotechnology, University of Science and Technology, Daejeon, Korea
[4]Department of Radiation Oncology, Asan Medical Center and University of Ulsan College of Medicine, Seoul, Korea

Corresponding author: Jae Bum Kim, jaebkim@snu.ac.kr.

Received 12 January 2016 and accepted 24 May 2016.

This article contains Supplementary Data online at http://diabetes.diabetesjournals.org/lookup/suppl/doi:10.2337/db16-0060/-/DC1.

M.H. and S.S.C. contributed equally to this work.

© 2016 by the American Diabetes Association. Readers may use this article as long as the work is properly cited, the use is educational and not for profit, and the work is not altered. More information is available at http://diabetesjournals.org/site/license.

processes related to ROS scavenging tend to be suppressed (9,10). Accordingly, treatment with NADPH oxidase inhibitors as well as antioxidant drugs attenuates ROS production and adipokine dysregulation, alleviating metabolic disorders such as insulin resistance in obesity (9,12). Thus it is likely that the imbalance between ROS production and scavenging in obese adipose tissue is closely associated with elevated adipose tissue inflammation and metabolic dysregulation.

Glucose-6-phosphate dehydrogenase (G6PD), a key enzyme of the pentose phosphate pathway, which shunts from the glycolytic pathway, catalyzes the synthesis of ribose for nucleic acid production and produces cytosolic NADPH (13). NADPH is one of the crucial cofactors that serve as a reducing equivalent in many metabolic pathways such as fatty acid and cholesterol biosynthesis (10). Moreover, G6PD plays a critical role in the regulation of the cellular redox potential by supplying the cofactor NADPH to ROS-producing and scavenging enzymes such as NADPH oxidase and glutathione reductase, respectively (10,13). In pathological conditions such as atherosclerosis, heart failure, and obesity, G6PD promotes cellular ROS production and proinflammatory signaling through increased availability of NADPH to ROS-producing enzymes (14–19). On the other hand, in various cell types, including erythrocytes, cardiomyocytes, endothelial cells, and pancreatic β-cells, G6PD contributes to the clearance of cellular oxidative stress by NADPH-dependent ROS-scavenging enzymes (20–23). We recently demonstrated that G6PD is highly expressed in the adipose tissues of obese and diabetic subjects (14,24). The aberrant upregulation of G6PD in adipose tissue leads to the dysregulation of lipid metabolism and adipokines and thus impairs insulin signaling in adipocytes (14,15). Furthermore, overexpression of G6PD in macrophages promotes oxidative stress and the expression of proinflammatory cytokines, which induce insulin resistance in adipocytes (24). Similarly, upregulation of G6PD in the liver, heart, and pancreatic β-cells of obese and diabetic animals also increases oxidative stress, which leads to functional defects in the respective tissues (12,25,26). Altogether, these findings suggest that anomalous G6PD upregulation in obese conditions might deteriorate energy homeostasis and oxidative stress, thereby accelerating metabolic complications.

G6PD deficiency is a common enzymopathy, affecting over 400 million people worldwide (13). One of the distinctive characteristics of patients with G6PD deficiency is hemolytic anemia, which is triggered by exposure to oxidative stress. As a potential animal model of human G6PD deficiency, a G6PD-deficient mutant ($G6PD^{mut}$) mouse model has been developed, which shows 10–15% of regular G6PD activity because of a reduction in G6PD protein expression by a splicing defect (27,28). Since the embryoprotective role of G6PD has been reported (20,29), various effects of G6PD deficiency on metabolic processes, immune responses, and organ development have been studied in $G6PD^{mut}$ mice (17,18,21,22,30). Furthermore, G6PD deficiency affects albuminuria and diet-induced cardiometabolic aberrations in $G6PD^{mut}$ mice (31,32). However, the effects of a G6PD defect in vivo on chronic inflammation and systemic insulin resistance in diet-induced obesity (DIO) still remain to be elucidated.

In this study we showed that $G6PD^{mut}$ mice exhibit improved glucose tolerance and reduced systemic insulin resistance in DIO. In the adipose tissue of $G6PD^{mut}$ mice fed a high-fat diet (HFD), the expression of NADPH oxidase and inflammatory cytokines was relieved, and the numbers of crown-like structures (CLSs) and infiltrated macrophages also diminished. Furthermore, proinflammatory responses were attenuated in the macrophages of $G6PD^{mut}$ mice, thus improving insulin signaling in adipocytes and hepatocytes. In line with these results, a transplant of $G6PD^{mut}$ bone marrow led to protection from diet-induced adipose tissue inflammation in wild-type (WT) recipient mice. Taken together, these data suggest that macrophage G6PD deficiency would mediate to lessen systemic insulin resistance in obesity by relieving proinflammatory signaling upon metabolic stresses.

RESEARCH DESIGN AND METHODS

Animals and Treatment

$G6PD^{mut}$ mice were provided by R. Matsui. $G6PD^{mut}$ (C3H) mice were backcrossed with C57BL/6 mice (Central Laboratory Animal Inc., Seoul, South Korea) more than 10 times to change the genetic background (Supplementary Fig. 1). The mice were genotyped by PCR (17), as illustrated in Supplementary Fig. 1. $G6PD^{mut}$ mice and their littermates were maintained on a normal chow diet (ND) until 8 weeks of age before being switched to a 60% HFD. For the oral or intraperitoneal glucose tolerance test, the mice were fasted for 6 h and basal blood samples were collected, then glucose was administered (2 g/kg body weight). Blood samples were drawn 15, 30, 60, 90, and 120 min after glucose administration to measure the glucose concentration. For the insulin tolerance test, the mice were fasted for 3 h and then insulin was administered (0.75 unit/kg body weight; Lilly, Indianapolis, IN); then blood glucose concentrations were measured at the indicated time points. To test in vivo insulin signaling, the mice were euthanized 20 min after a PBS or insulin injection (0.75 unit/kg body weight), and adipose tissues and livers were excised and quickly frozen for Western blot analysis. For a bone marrow transplant (BMT), 8-week-old recipient (C57BL/6) mice were lethally irradiated two times (total, 5 Gy) by means of a ^{137}Cs source at an interval of 4 h. After 4 h, these mice received a transplant of 5×10^6 bone marrow cells from $G6PD^{mut}$ mice or their WT littermates via tail vein injection, as previously described (33). ELISA kits for TNF-α, MCP-1 (Invitrogen, Grand Island, NY), and adiponectin (MIoBS, Japan) were used to measure their concentrations in protein extract of epididymal adipose tissue and serum. All animal procedures were conducted in accordance with the research guidelines of the Seoul National University Institutional Animal Care and Use Committee.

Isolation of Peritoneal Macrophages

Peritoneal macrophages were isolated from WT and G6PD^{mut} mice, as previously described (24). To detect lipopolysaccharide (LPS)–induced inflammatory signaling, peritoneal macrophages from WT and G6PD^{mut} mice were treated with LPS (10 ng/mL; Sigma-Aldrich, St. Louis, MO) for 30 min, and then the cells were harvested for Western blot analyses. For analysis of the expression of proinflammatory cytokines, the macrophages were incubated with LPS for 24 h.

Adipose Tissue Fractionation

Adipose tissue was fractionated as described previously (34). Briefly, epididymal adipose tissues (EATs) of HFD-fed WT and G6PD^{mut} mice were digested with type I collagenase buffer and filtered through a nylon mesh. After centrifugation, fractions of floating adipocytes and pelleted stromal vascular cells (SVCs) were washed several times with PBS and then used for RNA extraction.

Cell Culture and Conditioned Medium Experiment

3T3-L1 preadipocytes were grown in DMEM (HyClone, Logan, UT) supplemented with 10% bovine calf serum (HyClone). 3T3-L1 preadipocytes were differentiated as described previously (35). H4IIE hepatoma cells were grown in DMEM supplemented with 10% FBS (HyClone). For the conditioned medium (CM) experiment, peritoneal macrophages from WT and G6PD^{mut} mice were incubated in serum-free DMEM for 24 h, and CM was collected. Fully differentiated 3T3-L1 adipocytes and H4IIE hepatoma cells were incubated with CM for 24 h. To monitor insulin signaling, these cells were stimulated with insulin (100 nmol/L) for 30 min. To determine the expression level of gluconeogenic genes, H4IIE cells were stimulated with insulin (100 nmol/L) for 8 h. Insulin-stimulated glucose uptake by 3T3-L1 adipocytes was assessed by measuring [^{14}C]-2-deoxy-D-glucose uptake, as described previously (34).

Western Blot Analysis

Western blot analysis was performed as described previously (34). In brief, EAT, the liver, peritoneal macrophages, 3T3-L1 adipocytes, and H4IIE cells were lysed with NETN buffer. Nuclear extracts from macrophages were isolated as described previously (15). Cytosolic and membrane fractions from adipose tissues were prepared using a Proteo Extract Native Membrane Protein Extraction Kit (Merck Millipore, Germany) according to the manufacturer's protocol. The proteins were separated by SDS-PAGE and transferred to polyvinylidene fluoride membranes. The blots were probed with the following primary antibodies: anti-adiponectin, anti-G6PD, anti-lamin B, anti-pan-cadherin (Abcam, Cambridge, MA); anti-β-actin, anti-GAPDH (Sigma-Aldrich); anti-catalase, anti–superoxide dismutase 2 (Bethyl Laboratories, Montgomery, TX); anti-phospho (p)-AKT (Ser473), anti–fatty acid synthase, anti-p-GSK3β (Ser9), anti-p-JNK, anti-p65, anti-p50 (Cell Signaling Technology, Danvers, MA); anti-AKT, anti-GSK3β, anti-p-p38, anti-p67^{phox}, anti-SREBP1c (BD Biosciences); anti-NOX2 (Merck Millipore); anti-JNK, anti-p38, anti-p47^{phox}, and anti-SCD (Santa Cruz Biotechnology, Dallas, TX).

Quantitative RT-PCR

Total RNA was isolated from EAT, the liver, peritoneal macrophages, and H4IIE cells, then quantitative real-time RT-PCR was performed, as described previously (36). The primers were synthesized by Bioneer (Daejeon, South Korea), and their sequences are provided in Supplementary Table 1.

Immunohistochemistry

Whole-mount immunohistochemical analysis of EAT was performed as previously described (24). Whole-mounted EATs were incubated with primary antibodies against G6PD (1:500 dilution; Abcam), perilipin (1:1000; Fitzgerald, Acton, MA), CD11b (1:1000), and CD11c (1:1000; eBioscience, San Jose, CA). After incubation with fluorescently labeled secondary antibodies (Thermo Fisher Scientific, Waltham, MA) and DAPI (Vector Laboratories, Burlingame, CA) staining, the samples were examined under a Zeiss LSM 510-NLO confocal microscope. Slices cut from paraffin-embedded EATs were deparaffinized in xylene and rehydrated in a graded series of ethanol solutions. Endogenous peroxidase was inactivated using 3% hydrogen peroxide in methanol for 5 min. After blocking the slices with 10% horse serum, sections were incubated with a primary antibody against G6PD (1:100). The slices were incubated with horseradish peroxidase–conjugated secondary antibodies (Thermo Fisher Scientific) and visualized with 3,3′-diaminobenzidine (Vector Laboratories). Hematoxylin was used for counterstaining.

Measurement of Cellular ROS Levels

Cellular ROS was measured using chloromethyl-2′, 7′-dichlorodihydrofluorescein diacetate (H_2DCFDA) (Invitrogen). Peritoneal macrophages from WT and G6PD^{mut} mice were incubated with LPS for 30 min and then with DCFDA in the dark for 20 min. After a wash, fluorescent signals were detected using a confocal microscope.

Statistical Analysis

The results represent data from multiple independent experiments. Error bars in the figures denote the SD, and *P* values were calculated using the Student *t* test.

RESULTS

G6PD^{mut} Mice Exhibit Lower Levels of Fasting Insulin in HFD-Induced Obesity

It has been demonstrated that upregulated G6PD in obese adipose tissue contributes to inflammatory signaling via potentiating oxidative stress (10,15,24). However, it is not thoroughly understood whether genetic G6PD defect may alter adipose tissue inflammation and insulin resistance in obese animals. To address this, we investigated various aspects of DIO in G6PD^{mut} mice that were created by N-ethyl-N-nitrosourea (ENU) mutagenesis from *C3H* strain (27). To exclude off-target effects of random mutagenesis and the defective Toll-like receptor 4 (TLR4)–mediated inflammatory response in the *C3H/HeJ* strain

(37–41), the genetic background of G6PD^{mut} mice was changed to *C57BL/6* by backcross breeding more than 10 times with WT *C57BL/6* mice (Supplementary Fig. 1). Afterward, G6PD^{mut} mice were fed either an ND or HFD for 12 weeks and were compared with their WT littermates. As shown in Fig. 1*A–D*, HFD increased body weight, adipose tissue weight, and adipocyte size in both WT and G6PD^{mut} mice. In a *C57BL/6* background, the HFD challenge induced hyperglycemia in both WT and G6PD^{mut} mice (Fig. 1*E*). On the contrary, fasting insulin concentration and HOMA–insulin resistance (HOMA-IR) index, a quantitative analysis to measure insulin resistance, were significantly lower in HFD-fed G6PD^{mut} mice compared with HFD-fed WT mice (Fig. 1*F* and *G*). In addition, HFD-fed G6PD^{mut} mice showed decreased serum concentrations of free fatty acids that are readily released in insulin-resistant adipocytes (Fig. 1*H*).

HFD-Fed G6PD^{mut} Mice Show Ameliorated Insulin Resistance

Given that HFD-fed G6PD^{mut} mice exhibited reduced fasting insulin and HOMA-IR index, we hypothesized that the G6PD defect may be involved in the regulation of systemic insulin sensitivity in DIO. To test this, oral glucose tolerance and insulin tolerance tests were performed with WT and G6PD^{mut} mice. Under ND feeding, both WT and G6PD^{mut} mice showed similar glucose tolerance. Interestingly, HFD-fed G6PD^{mut} mice were more glucose and insulin tolerant than HFD-fed WT mice (Fig. 2*A* and *B*), which is consistent with the hypothesis that the reduction of fasting insulin concentration might be a result of improved insulin resistance in HFD-fed G6PD^{mut} mice. Next, to explore whether G6PD deficiency in DIO may influence insulin sensitivity in metabolic organs, the insulin signaling cascade was examined in the adipose tissue and liver of WT and G6PD^{mut} mice. As shown in Fig. 2*C*, compared with HFD-fed WT mice, in the adipose tissue of HFD-fed G6PD^{mut} mice, insulin-stimulated phosphorylation of AKT and GSK3β was significantly enhanced. Similarly, G6PD^{mut} mice also showed enhanced insulin signaling in the liver (Fig. 2*D*). Therefore, these observations indicated that G6PD deficiency would be associated with improved insulin resistance in DIO.

Expression of NADPH Oxidase Is Reduced in the Adipose Tissue of HFD-Fed G6PD^{mut} Mice

It has been reported that G6PD controls the redox balance by supplying the cofactor NADPH (15,24). NADPH oxidase is one of the major enzymes in NADPH-dependent ROS production, and its mRNA expression is upregulated in response to oxidative stress in obese adipose tissue (9). To determine whether a G6PD defect may attenuate the increased ROS production in DIO, the expression of NADPH oxidase subunits was examined in HFD-fed WT and G6PD^{mut} mice. As shown in Fig. 3*A* and *B*, both mRNA and protein

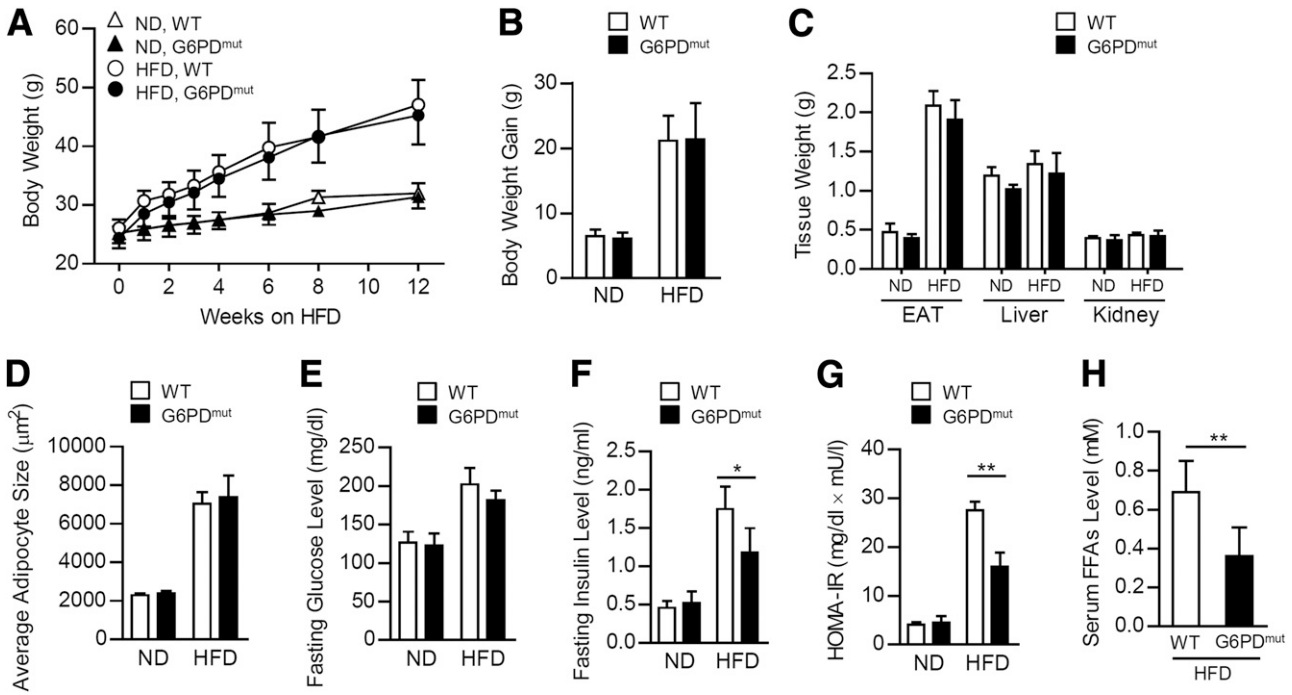

Figure 1—Fasting insulin and free fatty acids are decreased in HFD-fed G6PD^{mut} mice. G6PD^{mut} mice and their WT littermates (n = 6 per group) were fed either an ND or HFD for 12 weeks. *A*: Body weight was measured during the experimental periods. *B* and *C*: The body weight gain (*B*) and weights of various tissues (*C*) of WT and G6PD^{mut} mice were measured after 12 weeks of ND or HFD feeding. *D*: Average size of adipocytes was measured in the images of EAT slices. *E–H*: Fasting serum glucose (*E*) and insulin (*F*), HOMA-IR (*G*), and serum free fatty acids (FFAs) (*H*) in WT and G6PD^{mut} mice. The data represent the mean ± SD. *P < 0.05 and **P < 0.01 vs. WT group, Student t test.

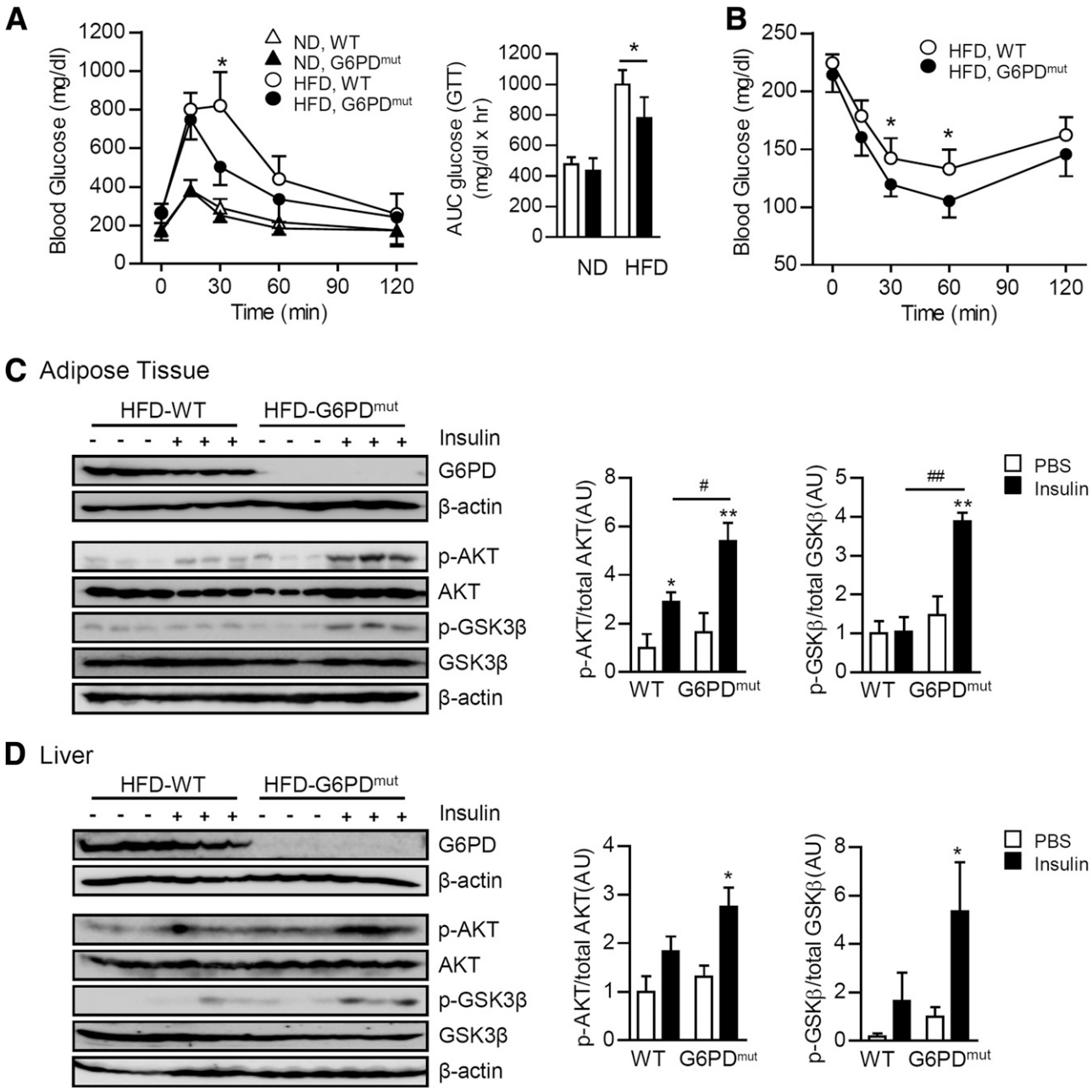

Figure 2—Insulin resistance is improved in HFD-fed G6PD^{mut} mice. *A* and *B*: Oral glucose tolerance test (GTT) and area under the curve (AUC) analysis (*A*) and insulin tolerance test (*B*) were performed on WT and G6PD^{mut} mice (n = 6 per group) fed an ND or HFD for 12 weeks. The data represent the mean ± SD. *P < 0.05 vs. WT group at each time point, Student t test. *C* and *D*: Insulin signaling in the EAT (*C*) and liver (*D*) of HFD-fed WT and G6PD^{mut} mice injected with saline or insulin (0.75 units/kg body weight) was analyzed by immunoblotting with antibodies against p-AKT, total AKT, p-GSK3β, and total GSK3β. β-Actin was used as the loading control. AU, arbitrary units. Quantitative data on the ratio of p-AKT and total AKT and the ratio of p-GSK3β and total GSK3β are represented as mean ± SD. *P < 0.05 and **P < 0.01 vs. no insulin control; #P < 0.05 and ##P < 0.01 vs. WT group, Student t test.

levels of NADPH oxidase subunits such as NOX2, p22^{phox}, p47^{phox}, and p67^{phox} were diminished in the adipose tissue of HFD-fed G6PD^{mut} mice compared with that of HFD-fed WT mice. By contrast, mRNA and protein levels of antioxidant genes including superoxide dismutase 2, catalase, and glutathione peroxidase were higher in the adipose tissue of G6PD^{mut} mice than that of WT mice with HFD feeding (Fig. 3*A* and *B*). It has been demonstrated that membrane translocation of cytosolic regulatory subunits such as p47^{phox} and p67^{phox} is required for activation of NADPH oxidase 2 (9). Compared with HFD-fed WT mice, the levels of p47^{phox} and p67^{phox} in the membrane fraction were also slightly decreased in HFD-fed G6PD^{mut} mice (Fig. 3*C*), implying that an active NADPH oxidase complex might

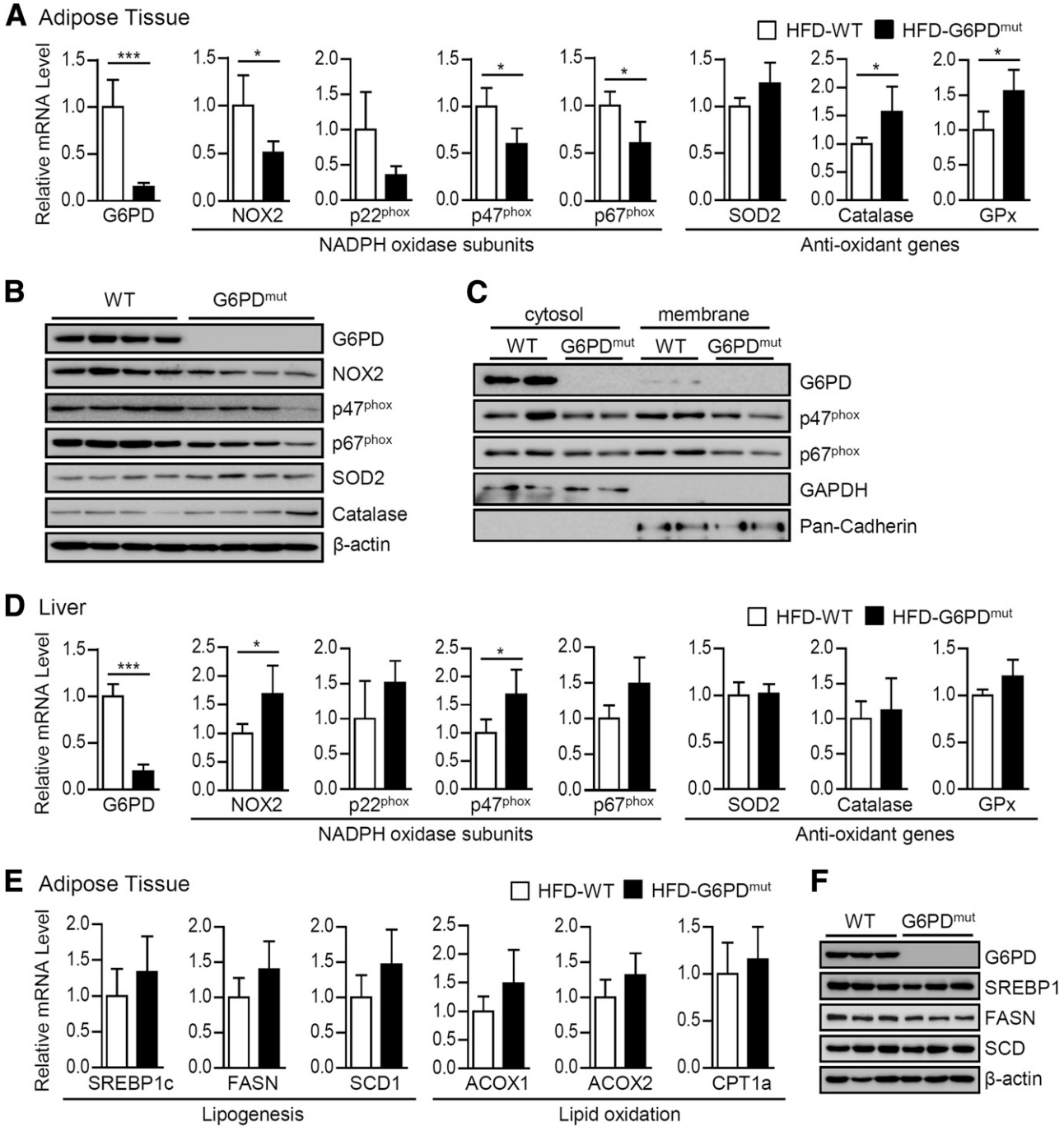

Figure 3—HFD-fed G6PD^{mut} mice exhibit downregulated expression of NADPH oxidase in adipose tissue. *A* and *B*: In EAT of HFD-fed WT and G6PD^{mut} mice (n = 6 per group), relative mRNA and protein levels of G6PD, NADPH oxidase subunits (NOX2, p22^{phox}, p47^{phox}, and p67^{phox}), and antioxidant genes were analyzed. *C*: To monitor the translocation of p47^{phox} and p67^{phox} into the membrane, cytosolic and membrane fractions from adipose tissue of HFD-fed WT and G6PD^{mut} mice were subjected to Western blot analysis. *D*: Relative mRNA levels of G6PD, NADPH oxidase subunits, and antioxidant genes in liver. *E* and *F*: Relative mRNA of lipogenic genes and oxidation genes (*E*) and protein levels of lipogenic genes (*F*) in adipose tissue. β-Actin was used as the loading control, and GAPDH and pan-cadherin were used as a cytosolic marker and a membrane marker, respectively. The data represent the mean ± SD. *P < 0.05 and ***P < 0.001 vs. WT group, Student t test. SOD2, superoxide dismutase 2; GPx, glutathione peroxidase; SREBP1c, sterol regulatory element–binding protein 1c; FASN, fatty acid synthase; SCD1, stearoyl-CoA desaturase 1; ACOX, acyl-CoA oxidase; CPT1a, carnitine palmitoyltransferase 1a.

be diminished by a G6PD defect in obese adipose tissue. Thus this finding indicated that oxidative stress would be decreased in the adipose tissue of HFD-fed G6PD^{mut} mice. On the other hand, suppression of NADPH oxidase and elevation of antioxidant genes by G6PD deficiency were not observed in the liver of the obese animals (Fig. 3*E*). These results implied that G6PD defect might selectively reduce oxidative stress in the adipose tissue of obese animals.

Adiposity and Fatty Liver Are Not Alleviated in HFD-Fed G6PD^{mut} Mice

In addition to redox regulation, G6PD is also involved in lipogenesis (14). Unexpectedly, we did not detect any reduction in adiposity in G6PD^{mut} mice compared with WT mice upon both ND and HFD feeding (Fig. 1). In addition, mRNA and protein levels of lipogenic genes such as sterol regulatory element-binding protein 1c, fatty acid synthase, and stearoyl-CoA desaturase 1, and mRNA level of lipid oxidation–related genes including acyl-CoA oxidase 1 and 2 and carnitine palmitoyltransferase 1a, in the adipose tissue of HFD-fed G6PD^{mut} mice were not different from those of HFD-fed WT mice (Fig. 3*E* and *F*). Furthermore, the levels of serum triglycerides and cholesterol were similar between WT and G6PD^{mut} mice (Supplementary Fig. 2*A* and *B*). WT and G6PD^{mut} mice showed a similar degree of nonalcoholic fatty liver upon HFD feeding. There was no difference in their morphological features (hematoxylin and eosin [H&E] staining), lipid contents (oil-red O staining), and tissue triglyceride levels in the liver of WT and G6PD^{mut} mice (Supplementary Fig. 2*C* and *D*). In addition, the expression of hepatic lipogenesis and lipid oxidation–related genes was not different between WT and G6PD^{mut} mice (Supplementary Fig. 2*E*).

Adipose Tissue Inflammation Is Attenuated in HFD-Fed G6PD^{mut} Mice

To test whether the improved insulin resistance of HFD-fed G6PD^{mut} mice might be associated with adipose tissue inflammation, macrophage accumulation was analyzed in the adipose tissue of WT and G6PD^{mut} mice under HFD feeding. As shown in Fig. 4*A* and *B*, HFD-fed G6PD^{mut} mice exhibited fewer CLSs and CD11c-positive proinflammatory macrophages (the classically activated M1 type) than HFD-fed WT mice did. Next, we examined gene expression profiles of proinflammatory cytokines and macrophage markers. Although there were no significant differences in the expression of proinflammatory genes between WT and G6PD^{mut} mice fed an ND (Supplementary Fig. 3), the mRNA level of CD11c was significantly reduced in the adipose tissue of HFD-fed G6PD^{mut} mice (Fig. 4*C*). In addition, both mRNA and protein levels of proinflammatory cytokines such as TNF-α and MCP-1 were decreased (Fig. 4*C* and *D*). On the contrary, mRNA and protein levels of adiponectin, a well-known anti-inflammatory adipokine, tended to be higher (Fig. 4*C* and *E*). Decreased expression of these inflammatory cytokines was more evident in the SVC fraction than in the adipocyte fraction isolated from adipose tissue of G6PD^{mut} mice (Fig. 4*F*). Additionally, the expression of M1 marker genes such as *CD11c* was significantly decreased in SVCs of G6PD^{mut} mice than those of WT mice fed an HFD (Fig. 4*G*). On the contrary, the expression of M2 marker genes such as *MGL1*, *MMR*, *Clec7a*, and *Ym1*, for anti-inflammatory macrophages (the alternatively activated M2 type) secreting anti-inflammatory cytokines, seemed to be slightly but not significantly increased in G6PD^{mut} mice (Fig. 4*G*). These data implied that M1 polarization of adipose tissue macrophages (ATMs) seemed to be partially attenuated in HFD-fed G6PD^{mut} mice. Furthermore, serum TNF-α and MCP-1 were reduced, whereas serum adiponectin was elevated in HFD-fed G6PD^{mut} mice compared with that in HFD-fed WT mice (Fig. 4*H*). Similar to the adipose tissues, mRNA levels of M1 markers (CD11c) and proinflammatory cytokines (TNF-α and MCP-1) were downregulated in the livers of HFD-fed G6PD^{mut} mice (Fig. 4*I*). Taken together, these results suggested that, in DIO, a G6PD defect would be protective against chronic inflammation, which is a key factor in boosting systemic insulin resistance.

G6PD Defect Suppresses Proinflammatory Responses in Macrophages

Accumulated ATMs are one of the key hallmarks of inflammation in obese adipose tissue, eventually leading to systemic insulin resistance (3). We previously demonstrated that macrophage G6PD modulates proinflammatory responses and oxidative stress, which are crucial stimuli for insulin resistance in adipocytes (24). Thus we decided to test whether a macrophage G6PD defect in G6PD^{mut} mice might indeed alter proinflammatory responses. To address this, peritoneal macrophages isolated from WT and G6PD^{mut} mice (Fig. 5*A*) were challenged with LPS, which is a potent initiator to provoke proinflammatory signals through TLR4. As shown in Fig. 5*B*, macrophages from G6PD^{mut} mice greatly attenuated phosphorylation of MAPKs such as p38 and JNK by LPS challenge. In addition, G6PD^{mut} macrophages exhibited decreased nuclear translocation of NF-κB, p65, and p50 upon LPS stimulation (Fig. 5*C*). Given that ROS in macrophages is one of the important signaling molecules participating in proinflammatory responses (7), we were prompted to test the levels of ROS in G6PD^{mut} macrophages. Compared with WT macrophages, macrophages from G6PD^{mut} mice showed reduced ROS accumulation in the presence of LPS (Fig. 5*D*). Moreover, the mRNA levels of TNF-α, IL-6, and MCP-1 genes were reduced in LPS-stimulated G6PD^{mut} macrophages (Fig. 5*E*). These data suggested that a macrophage G6PD defect would relieve oxidative stress and proinflammatory responses in G6PD^{mut} mice, which may lead to the suppression of adipose tissue inflammation in HFD-fed G6PD^{mut} mice.

Macrophage G6PD Deficiency Augments Insulin Action in Adipocytes and Hepatocytes

To test the idea that the attenuation of proinflammatory responses in G6PD^{mut} macrophages might affect insulin signaling in adipocytes and hepatocytes, 3T3-L1 adipocytes or H4IIE hepatoma cells were incubated with CM from LPS-stimulated WT or G6PD^{mut} macrophages. As shown in Fig. 6*A*, CM from WT macrophages decreased the phosphorylation of AKT and GSK3β in insulin-treated adipocytes, in contrast to the fresh medium. Unlike CM from WT macrophages, CM from G6PD^{mut} macrophages did not have such inhibitory effects on the insulin signaling

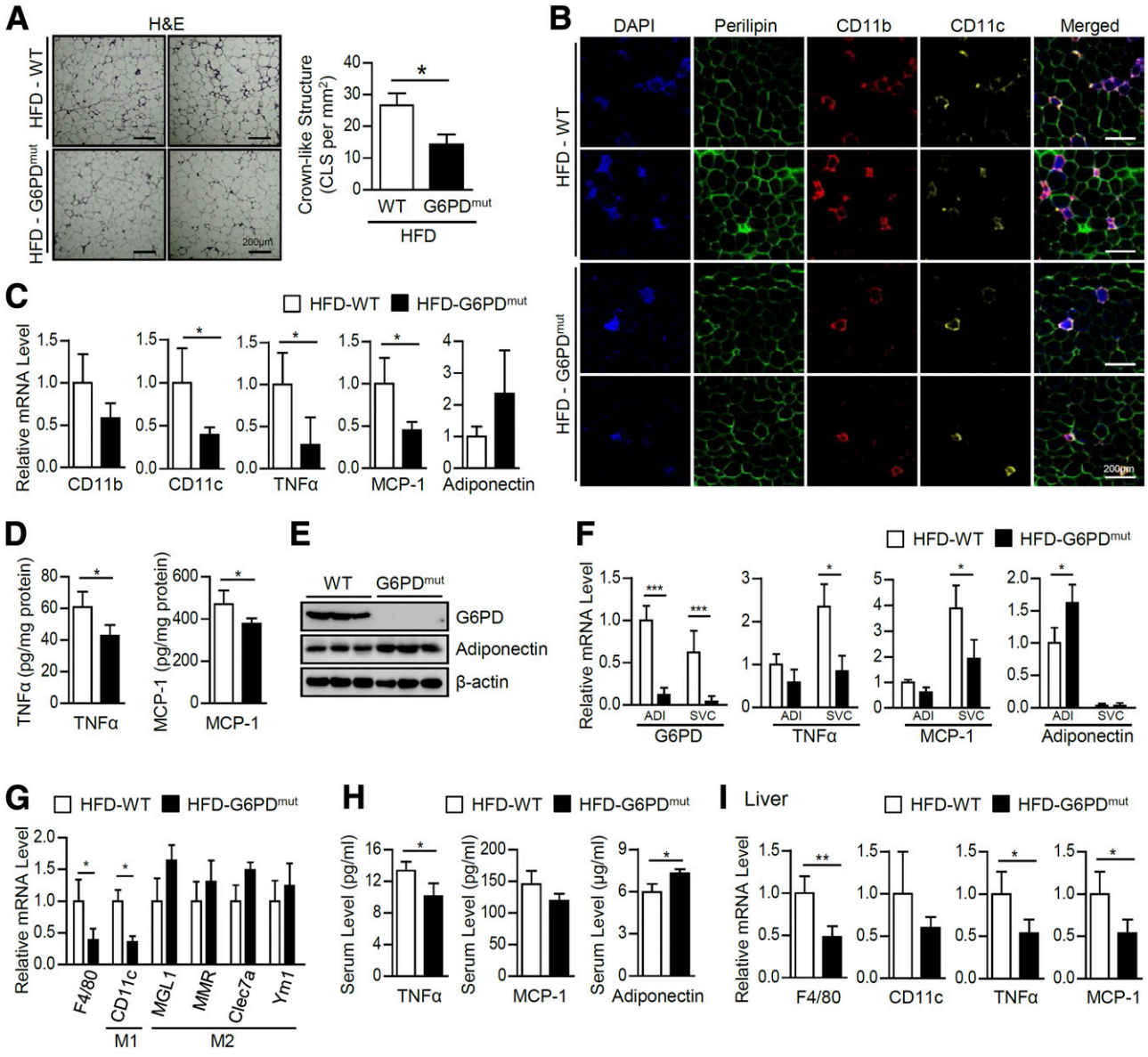

Figure 4—G6PD deficiency decreases chronic inflammation in adipose tissue and liver in DIO. *A* and *B*: Adipose tissue macrophage infiltration was detected in EAT from HFD-fed WT and G6PD^{mut} mice (n = 6 per group) through histological analysis via H&E staining (*A*) and whole-mount immunohistochemistry analysis of the nuclei (blue), perilipin (green), CD11b (red), and CD11c (yellow) (*B*). *C*–*E*: Relative mRNA levels of CD11b, CD11c, TNFα, MCP-1, and adiponectin (*C*) and protein levels of TNF-α, MCP-1, and adiponectin (*D* and *E*) were analyzed in EAT of HFD-fed WT and G6PD^{mut} mice; relative mRNA levels of G6PD, TNF-α, MCP-1, and adiponectin in adipocytes and SVCs fractionated from EATs (*F*); relative mRNA levels of marker genes of M1 and M2 macrophage in SVCs fractionated from EATs (*G*); serum TNF-α, MCP-1, and adiponectin (*H*); and relative mRNA levels of F4/80, CD11c, TNF-α, and MCP-1 in the liver (*I*). The data represent the mean ± SD. $^*P < 0.05$, $^{**}P < 0.01$, and $^{***}P < 0.001$ vs. WT group, Student t test.

cascade in insulin-treated adipocytes (Fig. 6*A*). In accordance with these results, CM from G6PD^{mut} macrophages restored the insulin-stimulated glucose uptake of adipocytes, which was inhibited by CM from WT macrophages (Fig. 6*B*). Just as in adipocytes, in H4IIE hepatoma cells, insulin signaling was also downregulated by CM from WT macrophages but not by CM from G6PD^{mut} macrophages (Fig. 6*C*). In addition, the mRNA levels of gluconeogenic genes such as glucose 6-phosphatase and phosphoenolpyruvate carboxylkinase were reduced in hepatoma cells upon insulin stimulation, which was partially reversed by CM from WT macrophages (Fig. 6*D*). In other words, it seems that CM from G6PD^{mut} macrophages did not interrupt insulin-driven suppression of gluconeogenic gene expression (Fig. 6*D*). These data implied that CM of WT macrophages may contain secretory factors that could inhibit insulin signaling or action in adipocytes and hepatocytes. Therefore our results suggested that macrophage G6PD deficiency might contribute to improve systemic insulin resistance in HFD-fed G6PD^{mut} mice.

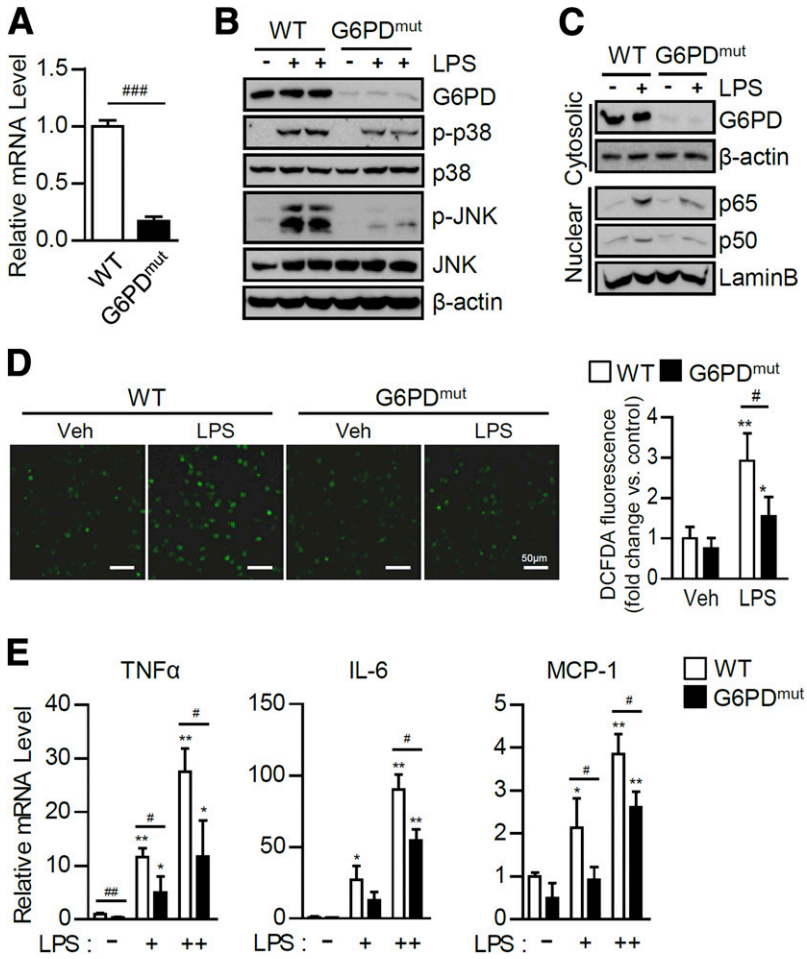

Figure 5—G6PD^{mut} macrophages exhibit attenuated proinflammatory responses. *A*: The relative mRNA level of G6PD was analyzed in peritoneal macrophages isolated from WT and G6PD^{mut} mice. *B* and *C*: WT and G6PD^{mut} macrophages were treated with LPS (10 ng/mL) for 30 min, and then total lysates were blotted and probed with antibodies to detect phosphorylation of p38 and JNK (*B*) and NF-κB (*C*). To detect translocated NF-κB subunits (p65 and p50) by LPS treatment, nuclear extracts were subjected to Western blot analysis. β-Actin and lamin B served as the loading control. *D*: In the absence or presence of LPS, the levels of cellular ROS in WT and G6PD^{mut} macrophages were measured and quantified using the redox-sensitive fluorescent dye chloromethyl-H_2DCFDA. Veh, vehicle control. *E*: After 24 h of LPS treatment, relative mRNA levels of proinflammatory cytokine genes such as TNF-α, IL-6, and MCP-1 were analyzed in WT and G6PD^{mut} macrophages. -, vehicle; +, 1 ng/mL LPS; ++, 10 ng/mL LPS. The data represent the mean ± SD. *P < 0.05, **P < 0.01 vs. LPS treatment; #P < 0.05, ##P < 0.01, and ###P < 0.001 vs. WT group, Student t test.

Hematopoietic G6PD Defect Ameliorates Glucose Intolerance in HFD-Induced Obesity

Given that macrophages from G6PD^{mut} mice exhibited attenuated proinflammatory response to LPS stimulation, we speculated that the deficiency of macrophage G6PD may be responsible for the relieved adipose tissue inflammation in HFD-fed G6PD^{mut} mice. To address this issue, a BMT was performed via adoptive transfer of bone marrow cells from G6PD^{mut} mice or their WT littermates into lethally irradiated *C57BL/6* WT mice. After that, WT mice that received the transplant of G6PD^{mut} bone marrow (G6PD^{mut} BMT) were fed an HFD for 16 weeks and compared with HFD-fed WT mice that received a transplant of WT bone marrow (WT BMT). As shown in Fig. 7*A*, genotyping analysis confirmed that bone marrow in G6PD^{mut} BMT mice was completely replaced with G6PD^{mut} cells. Also, G6PD^{mut} cells were partially present in the adipose tissue of HFD-fed G6PD^{mut} BMT mice, which seemed to derive from hematopoietic cells recruited from the replaced bone marrow cells (Fig. 7*A*). Immunohistochemical analysis revealed that G6PD in CD11c-positive ATMs of CLS was highly expressed in the obese adipose tissue of WT BMT mice, but its expression was clearly decreased in HFD-fed G6PD^{mut} BMT mice (Fig. 7*B*). Upon HFD feeding, there were no significant differences in body weight, adipose tissue weight, and adipocyte size between WT and G6PD^{mut} BMT mice (Fig. 7*C*–*F*). The fasting insulin concentration, however, was significantly lower in HFD-fed G6PD^{mut} BMT mice compared with HFD-fed WT BMT mice despite a similar fasting glucose concentration (Fig. 7*G* and *H*). In addition, HFD-fed G6PD^{mut} BMT mice were more glucose tolerant than HFD-fed WT BMT mice (Fig. 7*I*). Therefore

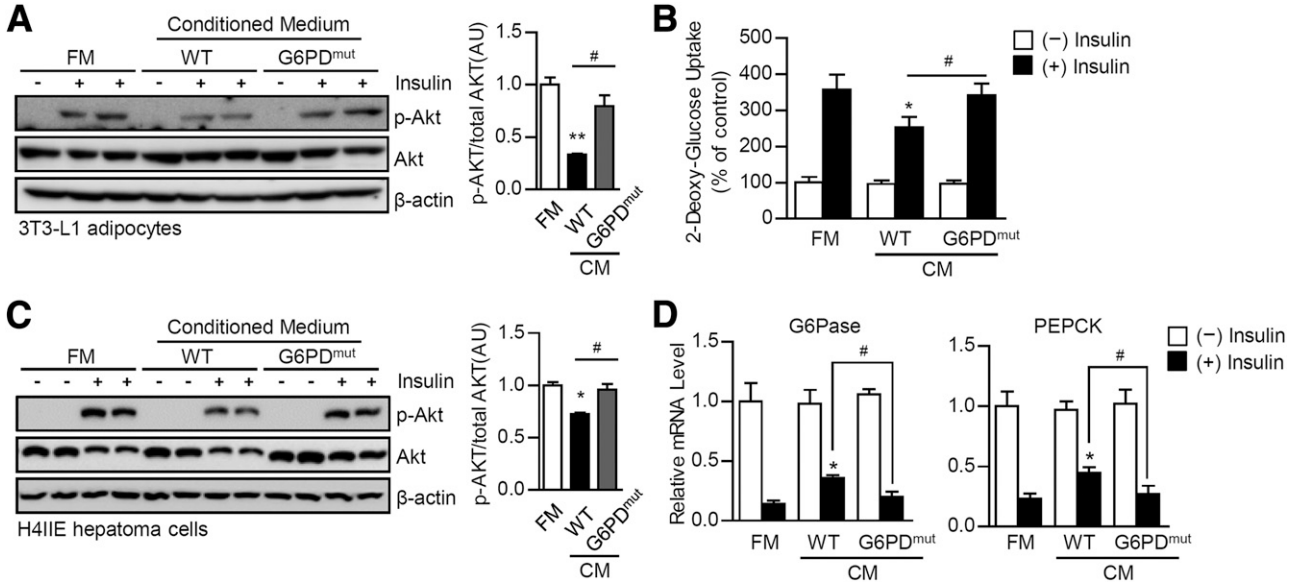

Figure 6—Macrophage G6PD deficiency improves insulin resistance in adipocytes and hepatocytes. *A* and *B*: Insulin-dependent phosphorylation of AKT (*A*) and glucose uptake (*B*) were analyzed in 3T3-L1 adipocytes treated with CM from WT and G6PD^{mut} macrophages. *C* and *D*: Insulin-dependent phosphorylation of AKT (*C*) and suppression of gluconeogenic genes such as glucose 6-phosphatase (G6Pase) and phosphoenolpyruvate carboxylkinase (PEPCK) (*D*) were analyzed in H4IIE hepatoma cells treated with CM from WT or G6PD^{mut} macrophages. β-Actin was used as the loading control. Quantitative data on the ratio of p-AKT and total AKT are represented as the mean ± SD. FM, fresh media. *$P < 0.05$ and **$P < 0.01$ vs. no treated control; #$P < 0.05$ vs. WT group, Student *t* test.

these data indicated that reconstitution of bone marrow in WT mice with G6PD^{mut} bone marrow could alleviate insulin resistance in DIO.

Hematopoietic G6PD Defect Protects Against Diet-Induced Adipose Tissue Inflammation

To explore whether adipose tissue inflammation might be associated with improved glucose tolerance in HFD-fed G6PD^{mut} BMT mice, macrophage accumulation was quantified in the adipose tissue of WT and G6PD^{mut} BMT mice with HFD. As shown in Fig. 8*A*, the numbers of CLSs were significantly decreased in the obese adipose tissue of G6PD^{mut} BMT mice compared with that of WT BMT mice. Similarly, HFD-fed G6PD^{mut} BMT mice showed downregulation of CD11c-positive proinflammatory macrophages in comparison with HFD-fed WT BMT mice (Fig. 8*B*). As expected, in WT mice the transplant of G6PD^{mut} bone marrow reduced the level of G6PD mRNA in adipose tissue in DIO (Fig. 8*C*). In addition, mRNA levels of NADPH oxidase subunits such as NOX2 and p22phox were decreased, whereas that of catalase was increased in the adipose tissue of HFD-fed G6PD^{mut} BMT mice, implying that the oxidative stress in the adipose tissue might be reduced by a hematopoietic G6PD defect (Fig. 8*C*). Furthermore, mRNA levels of proinflammatory cytokines such as TNF-α, IL-6, and MCP-1 were decreased, as was the expression of M1 marker genes such as *CD11c*. By contrast, the mRNA level of adiponectin tended to be increased (Fig. 8*D*). Taken together, these results suggest that hematopoietic G6PD deficiency would protect against HFD-induced adipose tissue inflammation, which might contribute to improve insulin resistance in G6PD^{mut} BMT mice.

DISCUSSION

NADPH-producing enzymes such as G6PD, malic enzyme (ME), and isocitrate dehydrogenase (IDH) play key roles in the regulation of the redox balance and in anabolic processes such as de novo lipid synthesis. In metabolic tissues such as adipose tissue and liver, dysregulation of these NADPH-producing enzymes has been implicated in metabolic disorders accompanied by chronic low-grade inflammation in obesity. For instance, it has been demonstrated that G6PD overexpression in adipocytes or macrophages potentiates inflammatory communications between adipocytes and macrophages, leading to insulin resistance in obesity (15,24). In addition, elevated G6PD expression in the adipose tissue of obese patients shows a positive correlation with various indicators of insulin resistance and macrophage accumulation (24). These findings raise the possibility that upregulated G6PD might be one of the mediators for adipose tissue inflammation in obesity. To test this hypothesis in an animal model, we investigated a G6PD^{mut} mouse model to decipher the pathophysiological roles of G6PD in obesity-induced metabolic complications.

It has been reported that severely G6PD-deficient embryos developed through G6PD-targeted homologous recombination are lethal because of damage in the central nervous system and heart on embryonic day 10.5 (29). Meanwhile, G6PD^{mut} mice developed through ENU random mutagenesis with *C3H* mice are viable and display no

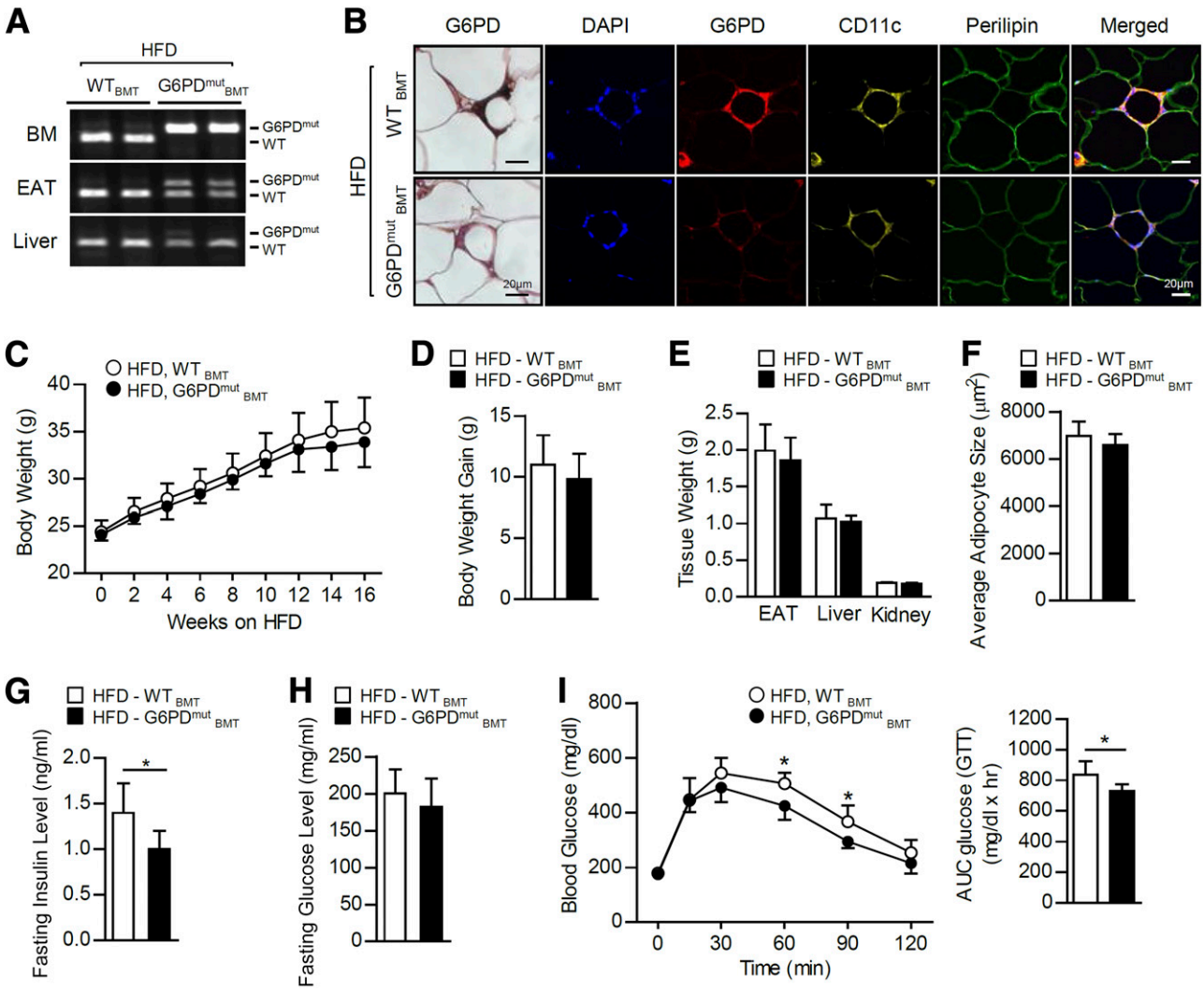

Figure 7—HFD-fed G6PD^{mut} BMT mice are glucose tolerant. WT and G6PD^{mut} BMT mice (n = 6 per group) were fed an HFD for 16 weeks. *A*: Genotyping analysis for WT (lower band) and G6PD mutation (upper band) was performed on genomic DNA from bone marrow (BM), EAT, and liver. *B*: Expression patterns of G6PD protein in ATMs of WT and G6PD^{mut} BMT mice were detected through immunohistochemical analysis of the G6PD (left, 3,3′-diaminobenzidine staining), nuclei (blue), G6PD (right, red), CD11c (yellow), and perilipin (green). *C*: Body weight was measured during the experimental periods. *D* and *E*: The body weight gain (*D*) and weights of various tissues (*E*) of WT and G6PD^{mut} BMT mice were measured after 16 weeks of HFD feeding. *F*: The average size of adipocytes was measured from images of EAT slices. *G–I*: Fasting serum insulin (*G*) and glucose (*H*) and intraperitoneal glucose tolerance test (GTT) and area under the curve (AUC) analysis (*I*) of HFD-fed WT and G6PD^{mut} BMT mice (n = 6 per group). The data represent the mean ± SD. *P < 0.05 vs. WT BMT group, Student t test.

apparent chronic hemolysis despite low G6PD activity (27). To date, G6PD^{mut} mice have been studied for various pathological conditions such as sepsis, teratogenesis, cardiovascular diseases, myocardial dysfunction, and atherosclerosis (17,18,20–22,30–32,42,43). Because of their genetic background, *C3H* G6PD^{mut} mice have some limitations for investigating obesity-mediated chronic inflammation and metabolic dysregulation. Accumulating evidence has suggested that different murine genetic backgrounds could affect diverse metabolic phenotypes such as susceptibility to DIO, hyperglycemia, insulin sensitivity, and proliferation and survival of β-cells, which lead to different experimental outcomes upon exposure to metabolic stresses (44,45). For example, it has been shown that the *C3H* strain is less susceptible to insulin resistance with increased insulin secretion and exhibits improved glucose metabolism (45). In addition, *C3H/HeJ* mice show defective endotoxin responses because of a mutation in the *TLR4* gene, which is a receptor essential for the induction of innate and adaptive immunity (37). Given that TLR4 signaling is activated by saturated free fatty acids as well as bacteria-derived glycolipids such as LPS (46), TLR4 plays key roles in obesity-associated disorders. Thus functional defects in TLR4 signaling in *C3H/HeJ* mice reduce adipose tissue inflammation in DIO, which is associated with insulin sensitivity and glucose metabolism (39–41). Consequently, we had to change the genetic background of G6PD^{mut} mice to *C57BL/6*, which would be a suitable model to study obesity-related metabolic

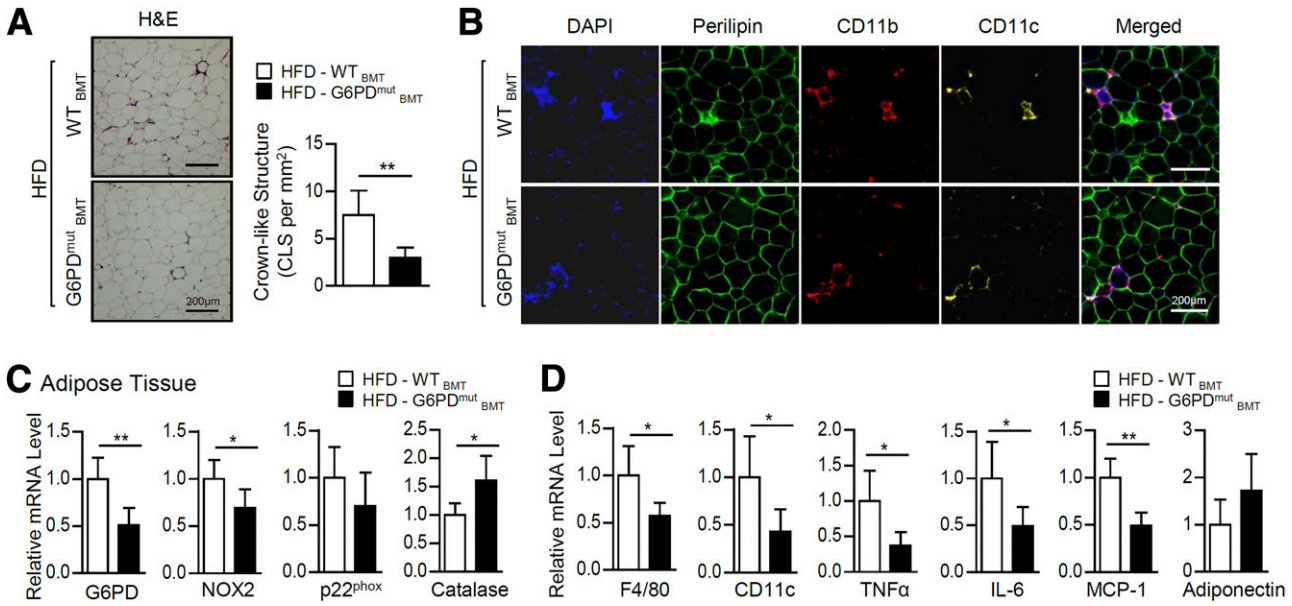

Figure 8—Adipose tissue inflammation is ameliorated in HFD-fed G6PD^{mut} BMT mice. *A* and *B*: Macrophage infiltration of adipose tissue was detected in the EAT of HFD-fed WT and G6PD^{mut} BMT mice (n = 6 per group) by histological analysis via H&E staining (*A*) and whole-mount immunohistochemistry analysis of the nuclei (blue), perilipin (green), CD11b (red), and CD11c (yellow) (*B*). *C*: Relative mRNA levels of G6PD, NADPH oxidase subunits (NOX2 and p22^{phox}), and catalase by quantitative RT-PCR in total RNA samples from EAT of HFD-fed WT and G6PD^{mut} BMT mice. *D*: Relative mRNA levels of F4/80, CD11c, TNF-α, IL-6, MCP-1, and adiponectin were analyzed in EAT. The data represent the mean ± SD. *P < 0.05 and **P < 0.01 vs. WT BMT group, Student t test.

disorders. Moreover, multiple rounds of backcrossing of G6PD^{mut} mice with *C57BL/6* mice should help to eliminate possible residual off-target effects during ENU chemical mutagenesis. With the *C57BL/6* background, G6PD^{mut} mice grew normally and were indistinguishable from age-matched WT littermates in spite of the reduced G6PD expression. Upon HFD feeding, G6PD^{mut} mice showed a body weight gain, hyperglycemia, and hyperinsulinemia in the *C57BL/6* background.

Without any metabolic stress such as an HFD, G6PD^{mut} mice exhibited a similar extent of glucose tolerance compared with WT mice. In DIO, however, G6PD^{mut} mice exhibited improved glucose tolerance and sensitized insulin signaling in peripheral tissues (Fig. 2). It was recently suggested that chronic low-grade inflammation in adipose tissue is one of the key factors that can exacerbate insulin resistance in obesity (1–3). In this work, several lines of evidence suggest that G6PD would exert substantial regulatory action on chronic inflammation in DIO. First, under HFD feeding, the expression of NADPH oxidase subunits was lower while that of antioxidant genes was higher in the adipose tissue of G6PD^{mut} mice compared with WT mice (Fig. 3). Unlike in adipose tissue, this gene expression profile was not altered in the livers of G6PD^{mut} mice. These results indicate that a G6PD defect could relieve oxidative stress, particularly in obese adipose tissue. Second, the population of CD11c-positive M1 ATMs was greatly reduced in adipose tissues of HFD-fed G6PD^{mut} mice (Fig. 4). In addition, the levels of several proinflammatory cytokines, including TNF-α and MCP-1, were decreased in adipose tissue and serum from HFD-fed G6PD^{mut} mice (Fig. 4). By contrast, adiponectin with anti-inflammatory and antidiabetic effects was elevated in adipose tissue and serum from HFD-fed G6PD^{mut} mice (Fig. 4). Moreover, G6PD^{mut} macrophages were resistant to proinflammatory stimulation by LPS (Fig. 5) and mediated enhanced insulin action in adipocytes and hepatocytes (Fig. 6), which were most likely driven by secretory factors from G6PD^{mut} macrophages. We recently reported that upregulated G6PD would induce the expression of proinflammatory cytokines by activation of NF-κB in adipose tissue (15,24). In obesity, secreted proinflammatory cytokines could further aggravate adipose tissue inflammation with promotion of M1 ATM recruitment as well as repress insulin action in adipose tissue by activating stress-activated kinases (4–6). Although the role of G6PD during macrophage polarization remains to be investigated, our recent data and previous reports have proposed that a G6PD defect in obesity might alleviate the vicious cycles between oxidative stress, proinflammatory response, and macrophage recruitment in adipose tissue. Therefore it is possible to speculate that G6PD deficiency in vivo would protect from systemic insulin resistance through the attenuation of chronic inflammation in obesity.

Studies on human G6PD deficiencies have suggested that G6PD would contribute to mediating immune cell functions (47–49). Severe human G6PD deficiency causes a chronic granulomatous disease with increased susceptibility to infections because of a defect in hydrogen peroxide production by granulocytes (47,48). Additionally, monocyte-derived

macrophages from subjects with G6PD-deficiency exhibit reduced secretion of inflammatory cytokines such as TNF-α and IL-1β (49). In agreement with these observations, we found that G6PD^{mut} macrophages showed reduced ROS production upon LPS stimulation in comparison with WT macrophages; this effect would eventually weaken the proinflammatory signaling and thereby suppress the induction of proinflammatory cytokines (Fig. 5). Additionally, in HFD-fed G6PD^{mut} BMT mice, hematopoietic G6PD deficiency attenuated the expression of proinflammatory cytokines and macrophage accumulation in adipose tissue, implying that G6PD in immune cells (that are recruited into adipose tissue) would be involved in inflammatory responses under metabolic stress (Fig. 8). Of course, it needs to be elucidated whether the reduced adipose tissue inflammation in HFD-fed G6PD^{mut} BMT mice might be mediated by other hematopoietic immune cells such as T lymphocytes, neutrophils, or eosinophils, as well as macrophages with G6PD deficiency. Nonetheless, our in vitro and in vivo data collectively indicate that macrophage G6PD deficiency at least would relieve chronic inflammation in HFD-fed G6PD^{mut} mice.

Although the transplant of G6PD^{mut} bone marrow into WT mice diminished the proinflammatory response in obese adipose tissue, we did not observe a marked reduction of proinflammatory cytokines or macrophage marker gene expression in the liver of HFD-fed G6PD^{mut} BMT mice (Supplementary Fig. 4). This phenomenon might be the result of rare infiltration of bone marrow–derived cells (with the G6PD^{mut} gene) into the liver of HFD-fed G6PD^{mut} BMT mice. Compared with the adipose tissues of HFD-fed G6PD^{mut} BMT mice, G6PD^{mut} cells were barely detectable in the liver according to PCR genotyping (Fig. 7*A*). In line with this finding, the level of G6PD mRNA was not reduced in the liver of HFD-fed G6PD^{mut} BMT mice (Supplementary Fig. 4). Although further studies are definitely needed to investigate the function of G6PD in Kupffer cells, our in vitro experiments (Fig. 6) propose the possibility that Kupffer cells with G6PD defect may influence proinflammatory response in the liver of mice with DIO.

In the process of de novo lipogenesis, NADPH is an essential cofactor that supplies reducing power for conversion of acetyl-CoA into fatty acids. Various NADPH-producing enzymes such as G6PD, ME, and IDH are abundantly expressed in adipose tissue (14). Given that NADPH production by G6PD is positively associated with lipogenic activity in adipocytes (14), we speculated that G6PD defect might affect the synthesis and/or accumulation of lipid metabolites in G6PD^{mut} mice. Unexpectedly, however, when compared with WT littermates, G6PD^{mut} mice did not show any changes in adiposity, fatty liver, serum triglycerides, and cholesterol upon ND or HFD feeding (Fig. 1 and Supplementary Fig. 2). The data indicating that serum free fatty acid levels were decreased in HFD-fed G6PD^{mut} mice (Fig. 1*H*) are probably the result of the augmented inhibitory effect of insulin on basal lipolysis with improved insulin sensitivity. Moreover, the expression of lipogenic genes was not altered in the adipose tissue and liver of WT and G6PD^{mut} mice (Fig. 3 and Supplementary Fig. 2). Currently, it is unclear why and how G6PD defect fails to influence adiposity or lipid metabolism. One of the putative explanations is a compensatory process driven by other NADPH-producing enzymes such as ME or IDH in G6PD^{mut} mice. It has been reported that NADP$^+$-dependent IDH, one of the IDH isoforms, can also mediate lipid biosynthesis in adipose tissue and liver via NADPH production (50). Transgenic mice overexpressing IDH show hyperlipidemia and marked lipid accumulation in adipose tissue and liver (50). On the other hand, we did not observe any change in the mRNA expression of other NADPH-producing enzymes such as ME and IDH in the adipose tissue and liver of HFD-fed G6PD^{mut} mice (Supplementary Fig. 5). Nevertheless, the possibility that these enzymes might be relatively activated in G6PD^{mut} mice cannot be excluded.

Here we showed that a genetic G6PD defect ameliorates chronic inflammation and insulin resistance in DIO. It is likely that inhibition of G6PD in obesity reduces cellular oxidative stress in adipose tissue, thus attenuating excessive proinflammatory responses and macrophage accumulation. Moreover, the attenuation of proinflammatory signaling by inhibiting G6PD may prevent chronic inflammation and systemic insulin resistance in obesity (Supplementary Fig. 6). Collectively, our data suggest that manipulation of G6PD activity may be a potential approach for countering obesity-induced metabolic disorders.

Acknowledgments. The authors thank R. Matsui for providing the G6PD^{mut} mice. The authors also thank Jong In Kim of Seoul National University for critically reading the manuscript.

Funding. This work was supported by the National Creative Research Initiative Program of the National Research Foundation (NRF) funded by the Korean government (the Ministry of Science, ICT & Future Planning, 2011-0018312). This research was also partly supported by the Bio & Medical Technology Development Program of the National Research Foundation (NRF) funded by the Ministry of Science, ICT & Future Planning (2012M3A9B6055344). K.C.S. was supported by the BK21 program.

Duality of Interest. No conflicts of interest relevant to this article were reported.

Author Contributions. M.H. and S.S.C. designed the study, performed experiments, and wrote the manuscript. K.C.S., G.C., J.-W.K., and J.-w.R. performed experiments and wrote the manuscript. J.-R.N., Y.-H.K., K.-H.Y., and C.-H.L. wrote the manuscript. J.B.K. supervised the whole project, discussed the data, and edited the final manuscript. J.B.K. is the guarantor of this work and, as such, had full access to all the data in this study and takes responsibility for the integrity of the data and the accuracy of the data analysis.

References

1. Olefsky JM, Glass CK. Macrophages, inflammation, and insulin resistance. Annu Rev Physiol 2010;72:219–246

2. Gregor MF, Hotamisligil GS. Inflammatory mechanisms in obesity. Annu Rev Immunol 2011;29:415–445

3. Chawla A, Nguyen KD, Goh YP. Macrophage-mediated inflammation in metabolic disease. Nat Rev Immunol 2011;11:738–749

4. Yuan M, Konstantopoulos N, Lee J, et al. Reversal of obesity- and diet-induced insulin resistance with salicylates or targeted disruption of Ikkbeta. Science 2001;293:1673–1677
5. Hirosumi J, Tuncman G, Chang L, et al. A central role for JNK in obesity and insulin resistance. Nature 2002;420:333–336
6. Gao Z, Zhang J, Kheterpal I, Kennedy N, Davis RJ, Ye J. Sirtuin 1 (SIRT1) protein degradation in response to persistent c-Jun N-terminal kinase 1 (JNK1) activation contributes to hepatic steatosis in obesity. J Biol Chem 2011;286: 22227–22234
7. Evans JL, Goldfine ID, Maddux BA, Grodsky GM. Oxidative stress and stress-activated signaling pathways: a unifying hypothesis of type 2 diabetes. Endocr Rev 2002;23:599–622
8. Yeop Han C, Kargi AY, Omer M, et al. Differential effect of saturated and unsaturated free fatty acids on the generation of monocyte adhesion and chemotactic factors by adipocytes: dissociation of adipocyte hypertrophy from inflammation. Diabetes 2010;59:386–396
9. Furukawa S, Fujita T, Shimabukuro M, et al. Increased oxidative stress in obesity and its impact on metabolic syndrome. J Clin Invest 2004;114:1752–1761
10. Park J, Chung JJ, Kim JB. New evaluations of redox regulating system in adipose tissue of obesity. Diabetes Res Clin Pract 2007;77(Suppl 1):S11–S16
11. Han CY, Umemoto T, Omer M, et al. NADPH oxidase-derived reactive oxygen species increases expression of monocyte chemotactic factor genes in cultured adipocytes. J Biol Chem 2012;287:10379–10393
12. Gupte RS, Floyd BC, Kozicky M, et al. Synergistic activation of glucose-6-phosphate dehydrogenase and NAD(P)H oxidase by Src kinase elevates superoxide in type 2 diabetic, Zucker fa/fa, rat liver. Free Radic Biol Med 2009;47:219–228
13. Cappellini MD, Fiorelli G. Glucose-6-phosphate dehydrogenase deficiency. Lancet 2008;371:64–74
14. Park J, Rho HK, Kim KH, Choe SS, Lee YS, Kim JB. Overexpression of glucose-6-phosphate dehydrogenase is associated with lipid dysregulation and insulin resistance in obesity. Mol Cell Biol 2005;25:5146–5157
15. Park J, Choe SS, Choi AH, et al. Increase in glucose-6-phosphate dehydrogenase in adipocytes stimulates oxidative stress and inflammatory signals. Diabetes 2006;55:2939–2949
16. Gupte SA, Levine RJ, Gupte RS, et al. Glucose-6-phosphate dehydrogenase-derived NADPH fuels superoxide production in the failing heart. J Mol Cell Cardiol 2006;41:340–349
17. Matsui R, Xu S, Maitland KA, et al. Glucose-6 phosphate dehydrogenase deficiency decreases the vascular response to angiotensin II. Circulation 2005; 112:257–263
18. Matsui R, Xu S, Maitland KA, et al. Glucose-6-phosphate dehydrogenase deficiency decreases vascular superoxide and atherosclerotic lesions in apolipoprotein E(-/-) mice. Arterioscler Thromb Vasc Biol 2006;26:910–916
19. Hecker PA, Leopold JA, Gupte SA, Recchia FA, Stanley WC. Impact of glucose-6-phosphate dehydrogenase deficiency on the pathophysiology of cardiovascular disease. Am J Physiol Heart Circ Physiol 2013;304:H491–H500
20. Nicol CJ, Zielenski J, Tsui LC, Wells PG. An embryoprotective role for glucose-6-phosphate dehydrogenase in developmental oxidative stress and chemical teratogenesis. FASEB J 2000;14:111–127
21. Jain M, Brenner DA, Cui L, et al. Glucose-6-phosphate dehydrogenase modulates cytosolic redox status and contractile phenotype in adult cardiomyocytes. Circ Res 2003;93:e9–e16
22. Zhang Z, Liew CW, Handy DE, et al. High glucose inhibits glucose-6-phosphate dehydrogenase, leading to increased oxidative stress and beta-cell apoptosis. FASEB J 2010;24:1497–1505
23. Leopold JA, Zhang YY, Scribner AW, Stanton RC, Loscalzo J. Glucose-6-phosphate dehydrogenase overexpression decreases endothelial cell oxidant stress and increases bioavailable nitric oxide. Arterioscler Thromb Vasc Biol 2003;23:411–417
24. Ham M, Lee JW, Choi AH, et al. Macrophage glucose-6-phosphate dehydrogenase stimulates proinflammatory responses with oxidative stress. Mol Cell Biol 2013;33:2425–2435
25. Serpillon S, Floyd BC, Gupte RS, et al. Superoxide production by NAD(P)H oxidase and mitochondria is increased in genetically obese and hyperglycemic rat heart and aorta before the development of cardiac dysfunction. The role of glucose-6-phosphate dehydrogenase-derived NADPH. Am J Physiol Heart Circ Physiol 2009;297:H153–H162
26. Lee JW, Choi AH, Ham M, et al. G6PD up-regulation promotes pancreatic beta-cell dysfunction. Endocrinology 2011;152:793–803
27. Pretsch W, Charles DJ, Merkle S. X-linked glucose-6-phosphate dehydrogenase deficiency in Mus musculus. Biochem Genet 1988;26:89–103
28. Sanders S, Smith DP, Thomas GA, Williams ED. A glucose-6-phosphate dehydrogenase (G6PD) splice site consensus sequence mutation associated with G6PD enzyme deficiency. Mutat Res 1997;374:79–87
29. Longo L, Vanegas OC, Patel M, et al. Maternally transmitted severe glucose 6-phosphate dehydrogenase deficiency is an embryonic lethal. EMBO J 2002;21: 4229–4239
30. Wilmanski J, Villanueva E, Deitch EA, Spolarics Z. Glucose-6-phosphate dehydrogenase deficiency and the inflammatory response to endotoxin and polymicrobial sepsis. Crit Care Med 2007;35:510–518
31. Xu Y, Zhang Z, Hu J, et al. Glucose-6-phosphate dehydrogenase-deficient mice have increased renal oxidative stress and increased albuminuria. FASEB J 2010;24:609–616
32. Hecker PA, Mapanga RF, Kimar CP, et al. Effects of glucose-6-phosphate dehydrogenase deficiency on the metabolic and cardiac responses to obesogenic or high-fructose diets. Am J Physiol Endocrinol Metab 2012;303:E959–E972
33. Joseph SB, Bradley MN, Castrillo A, et al. LXR-dependent gene expression is important for macrophage survival and the innate immune response. Cell 2004;119:299–309
34. Choe SS, Shin KC, Ka S, Lee YK, Chun JS, Kim JB. Macrophage HIF-2α ameliorates adipose tissue inflammation and insulin resistance in obesity. Diabetes 2014;63:3359–3371
35. Lee YS, Choi JW, Hwang I, et al. Adipocytokine orosomucoid integrates inflammatory and metabolic signals to preserve energy homeostasis by resolving immoderate inflammation. J Biol Chem 2010;285:22174–22185
36. Lee HW, Suh JH, Kim HN, et al. Berberine promotes osteoblast differentiation by Runx2 activation with p38 MAPK. J Bone Miner Res 2008;23:1227–1237
37. Poltorak A, He X, Smirnova I, et al. Defective LPS signaling in C3H/HeJ and C57BL/10ScCr mice: mutations in Tlr4 gene. Science 1998;282:2085–2088
38. Ye D, Li FY, Lam KS, et al. Toll-like receptor-4 mediates obesity-induced non-alcoholic steatohepatitis through activation of X-box binding protein-1 in mice. Gut 2012;61:1058–1067
39. Tsukumo DM, Carvalho-Filho MA, Carvalheira JB, et al. Loss-of-function mutation in Toll-like receptor 4 prevents diet-induced obesity and insulin resistance. Diabetes 2007;56:1986–1998
40. Poggi M, Bastelica D, Gual P, et al. C3H/HeJ mice carrying a toll-like receptor 4 mutation are protected against the development of insulin resistance in white adipose tissue in response to a high-fat diet. Diabetologia 2007;50:1267–1276
41. Suganami T, Mieda T, Itoh M, Shimoda Y, Kamei Y, Ogawa Y. Attenuation of obesity-induced adipose tissue inflammation in C3H/HeJ mice carrying a Toll-like receptor 4 mutation. Biochem Biophys Res Commun 2007;354:45–49
42. Leopold JA, Walker J, Scribner AW, et al. Glucose-6-phosphate dehydrogenase modulates vascular endothelial growth factor-mediated angiogenesis. J Biol Chem 2003;278:32100–32106
43. Spencer NY, Yan Z, Boudreau RL, et al. Control of hepatic nuclear superoxide production by glucose 6-phosphate dehydrogenase and NADPH oxidase-4. J Biol Chem 2011;286:8977–8987
44. Montgomery MK, Hallahan NL, Brown SH, et al. Mouse strain-dependent variation in obesity and glucose homeostasis in response to high-fat feeding. Diabetologia 2013;56:1129–1139
45. Kaku K, Fiedorek FT Jr, Province M, Permutt MA. Genetic analysis of glucose tolerance in inbred mouse strains. Evidence for polygenic control. Diabetes 1988;37:707–713

46. Shi H, Kokoeva MV, Inouye K, Tzameli I, Yin H, Flier JS. TLR4 links innate immunity and fatty acid-induced insulin resistance. J Clin Invest 2006;116:3015–3025

47. Cooper MR, DeChatelet LR, McCall CE, LaVia MF, Spurr CL, Baehner RL. Complete deficiency of leukocyte glucose-6-phosphate dehydrogenase with defective bactericidal activity. J Clin Invest 1972;51:769–778

48. Gray GR, Stamatoyannopoulos G, Naiman SC, et al. Neutrophil dysfunction, chronic granulomatous disease, and non-spherocytic haemolytic anaemia caused by complete deficiency of glucose-6-phosphate dehydrogenase. Lancet 1973;2:530–534

49. Sanna F, Bonatesta RR, Frongia B, et al. Production of inflammatory molecules in peripheral blood mononuclear cells from severely glucose-6-phosphate dehydrogenase-deficient subjects. J Vasc Res 2007;44:253–263

50. Koh HJ, Lee SM, Son BG, et al. Cytosolic NADP+-dependent isocitrate dehydrogenase plays a key role in lipid metabolism. J Biol Chem 2004;279:39968–39974